The background of the cover features a blue gradient with a molecular structure composed of white spheres connected by thin lines. A vertical orange bar is on the left side. There are some lens flare effects on the left side.

# Surface Chemistry of Tungsten Trioxide: A Theoretical Study

▶ Jin Hua



科学技术文献出版社  
SCIENTIFIC AND TECHNICAL DOCUMENTATION PRESS

# Surface Chemistry of Tungsten Trioxide: A Theoretical Study

by Jin Hua (金 华 著)

常州大学图书馆  
藏书章



科学技术文献出版社  
SCIENTIFIC AND TECHNICAL DOCUMENTATION PRESS

· 北京 ·

## 图书在版编目 (CIP) 数据

三氧化钨表面化学的理论研究 = Surface Chemistry of Tungsten Trioxide: A Theoretical Study: 英文 / 金华著. —北京: 科学技术文献出版社, 2018. 12

ISBN 978-7-5189-4706-5

I. ①三… II. ①金… III. ①氧化钨—表面化学—研究—英文 IV. ①O647.11

中国版本图书馆 CIP 数据核字 (2018) 第 169929 号

## Surface Chemistry of Tungsten Trioxide: A Theoretical Study

策划编辑: 张丹 责任编辑: 李鑫 马新娟 责任校对: 文浩 责任出版: 张志平

出版者 科学技术文献出版社

地址 北京市复兴路15号 邮编 100038

编务部 (010) 58882938, 58882087 (传真)

发行部 (010) 58882868, 58882870 (传真)

邮购部 (010) 58882873

官方网址 [www.stdp.com.cn](http://www.stdp.com.cn)

发行者 科学技术文献出版社发行 全国各地新华书店经销

印刷者 北京虎彩文化传播有限公司

版次 2018年12月第1版 2018年12月第1次印刷

开本 710×1000 1/16

字数 160千

印张 10.25

书号 ISBN 978-7-5189-4706-5

定价 48.00元



版权所有 违法必究

购买本社图书, 凡字迹不清、缺页、倒页、脱页者, 本社发行部负责调换

## PREFACE

Tungsten trioxide ( $\text{WO}_3$ ) is a kind of multifunctional semiconductor materials, and it has been widely used in different fields including photochromism, electrochromism, chemical sensors and so on, for its unique physical and chemical properties. In this work, the electronic structure and surface chemical reactivity of tungsten trioxide semiconductor are systematically investigated by using DFT method. It is hoped that this book would provide reliable theoretical foundation to get deep insight into the origin of the characteristic of  $\text{WO}_3$ -based material, as well as designing the new heterogeneous catalysts. The main conclusions of this book are as listed in following.

1. The structural and electronic properties of seven  $\text{WO}_3$  bulk phases have been studied. Our calculations indicate that, among these phases the simple cubic structure is the least stable, but the energy difference between different  $\text{WO}_3$  phases is small ( $< 0.1$  eV per  $\text{WO}_3$  unit). When the unit cell is distorted from the cubic structure, the reducing of the symmetry results in the increasing of the band gap. According to our theoretical results, the band gaps of simple cubic, tetragonal, hexagonal, orthorhombic, RT-monoclinic, triclinic, and LT-monoclinic phases are 1.42 eV, 1.46 eV, 1.55 eV, 2.13 eV, 2.47 eV, 2.54 eV and 2.75 eV, respectively.

2. Geometries and electronic structures of a series of reconstructed  $\text{WO}_3(001)$  surfaces have been systematically investigated. Our calculations demonstrate that the reconstructed  $(\sqrt{2} \times \sqrt{2})R45^\circ$  surface has the lowest surface energy and is thermodynamically most stable. According to the electronic structure, the bridging oxygen at surface is the main component of the top maximum of the valence band, while the contributions of the top oxygen atom locate at lower energy region. Comparing with the structural and electronic properties of a series of  $(\text{WO}_3)_n$  clusters,

the similarities in the structural and electronic properties between cluster and surface can be found when  $n = 6$ , thus  $W_6O_{18}$  can be viewed as the smallest molecular model to understand the complex processes happened on the  $WO_3$  surface.

3. The oxidation reactions of CO on perfect, defective and  $O_2$ -pre-adsorbed  $WO_3(001)$  have been systematically investigated. A possible full catalytic cycle is proposed to make the perfect  $WO_3(001)$  surface as catalyst for CO oxidation, which contains three steps: (a) CO reacts with the top oxygen of the perfect  $WO_3(001)$  surface to form a  $CO_2$  molecule and the corresponding defective surface is formed; (b) the  $O_2$  molecule is activated after adsorbing on the defective surface, because of the formation of  $O_2^{2-}$  species; (c) another CO molecule reacts with the pre-adsorbed  $O_2$  to form the second  $CO_2$  molecule, and meanwhile the initial perfect surface is subsequently regenerated. The NEB calculations indicate that all steps are exothermic strongly; however, the first step is the rate-limiting step from the kinetics viewpoint.

4. Geometries and electronic structures of  $WO_3(001)$  surface doped by VB, VIB, and VII B transition metals have been systematically explored. According to the doping energy, only the Ta doping is energetically favorable. By analyzing the electronic structures of four Ta-doped configurations, the distribution of terminal-oxygen radical as observed in  $W_3O_9^+$  can be reproduced only when a Ta atom replaces a six-coordinated W atom on the surface. After doping, the top oxygen just above Ta atom is activated, and the CO oxidation reaction on the  $WO_3(001)$  surface is enhanced. With respect to the undoped surface, the activation energy of the corresponding rate-determining step is reduced obviously about 0.64 eV.

In addition, we have also simulated the photo-oxidation mechanism of water on the  $WO_3$  surface by using positively charged and neutral  $W_6O_{18}$  cluster models. The results obtained by two models are consistent with each other, and the rate-limiting step for the water oxidation on the  $WO_3$  surface is related to the breaking of the O—H bond.

# CONTENT

<b>Chapter 1 Introduction</b>	1
1.1 Applications of Tungsten Trioxide	1
1.1.1 Coloration	1
1.1.2 Gas Sensors	3
1.1.3 Photo-catalytic Degradation	4
1.1.4 Water-splitting Electrode	4
1.2 Research Progress in $\text{WO}_3$ Bulk	6
1.3 Research Progress in $(\text{WO}_3)_n$ Clusters	9
1.4 Research Progress in $\text{WO}_3(001)$ Surface	11
1.4.1 Surface Configuration and Surface Energy	12
1.4.2 Electronic Structure	15
1.5 Research in CO Oxidation on $\text{WO}_3(001)$ Surface	18
1.6 Research Progress in Transition Metal-doped $\text{WO}_3(001)$ Surface	20
1.7 Research in Water Splitting on $\text{WO}_3(001)$ Surface	21
1.8 Research Objective	24
<b>Chapter 2 Geometry and Electronic Structures of <math>\text{WO}_3</math> Bulk</b>	26
2.1 Introduction	26
2.2 Computational Details	27
2.3 Results and Discussion	31
2.3.1 Structural and Electronic Properties of	113

RT-Monoclinic $\text{WO}_3$ .....	31
2.3.2 Structural and Electronic Properties of Simple Cubic $\text{WO}_3$ .....	36
2.3.3 Structural and Electronic Properties of Tetragonal $\text{WO}_3$ .....	38
2.3.4 Structural and Electronic Properties of LT-Monoclinic $\text{WO}_3$ .....	40
2.3.5 Structural and Electronic Properties of Orthorhombic $\text{WO}_3$ .....	42
2.3.6 Structural and Electronic Properties of Triclinic $\text{WO}_3$ .....	43
2.3.7 Structural and Electronic Properties of Hexagonal $\text{WO}_3$ .....	44
2.4 Conclusions .....	45

### Chapter 3 Geometry and Electronic Structures of $(\text{WO}_3)_n$ Clusters

$(n = 1 \sim 6)$ and $\text{WO}_3(001)$ Solid Surface .....	46
3.1 Introduction .....	46
3.2 Computational Details .....	47
3.3 Results and Discussion .....	49
3.3.1 Stability of Reconstructed Cubic $\text{WO}_3(001)$ Surfaces .....	49
3.3.2 Geometry of the Relaxed $(\sqrt{2} \times \sqrt{2})R45^\circ \text{WO}_3(001)$ Surface .....	53
3.3.3 Electronic Structure of the Relaxed $(\sqrt{2} \times \sqrt{2})R45^\circ$ $\text{WO}_3(001)$ Surface .....	56
3.3.4 STM Simulations of Reconstructed $\text{WO}_3(001)$ Surfaces .....	59
3.3.5 Comparisons Between $\text{WO}_3(001)$ Surface and the $(\text{WO}_3)_n$ Clusters .....	60
3.3.6 Adsorptions of $\text{BH}_3$ Molecule on $\text{WO}_3(001)$ Surface	

and $W_6O_{18}$ Cluster .....	64
3.4 Conclusions .....	67
<b>Chapter 4 Mechanism of CO Oxidation on <math>WO_3(001)</math> Surface</b> .....	69
4.1 Introduction .....	69
4.2 Computational Details .....	70
4.3 Results and Discussion .....	71
4.3.1 Surface Oxygen Species and Oxygen Vacancy on $WO_3(001)$ Surface .....	71
4.3.2 Adsorption of CO on $WO_3(001)$ Surface .....	78
4.3.3 Oxidation of CO on $WO_3(001)$ Surface .....	81
4.4 Conclusions .....	88
<b>Chapter 5 Geometry and Electronic Structures of Transition Metal-doped <math>WO_3(001)</math> Surface</b> .....	90
5.1 Introduction .....	90
5.2 Computational Details .....	92
5.3 Results and Discussion .....	93
5.3.1 Structures and Thermodynamic Stabilities of the <i>M</i> -doped $WO_3(001)$ Surfaces .....	93
5.3.2 Electronic Structures of the Ta-doped $WO_3(001)$ Surfaces .....	98
5.3.3 Oxidation of CO Molecule on the Ta- $W_{6f}$ Doped $WO_3(001)$ Surfaces .....	104
5.4 Conclusions .....	108
<b>Chapter 6 Photo-oxidation of Water on Tungsten Trioxide</b> .....	111
6.1 Introduction .....	111
6.2 Computational Details .....	112
6.2.1 Water-splitting Reactions .....	112
6.2.2 Methods .....	113

6.2.3	Models .....	115
6.3	Results and Discussion .....	118
6.3.1	Results for Method I .....	118
6.3.2	Results for Method II .....	120
6.4	Conclusions .....	123
<b>Chapter 7 Concluding Remarks .....</b>		<b>125</b>
<b>Appendix A Theoretical Background .....</b>		<b>129</b>
A.1	Density Functional Theory .....	129
A.2	Exchange and Correlation .....	132
A.3	Plane-wave Basis Set Combined with Atomic-orbital Basis Set .....	134
A.4	Scanning Tunneling Microscope .....	136
A.5	Work Function .....	138
<b>References .....</b>		<b>139</b>

# Chapter 1

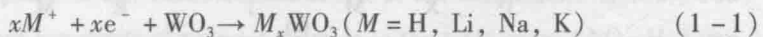
## Introduction

### 1.1 Applications of Tungsten Trioxide

Transition metal oxide is an important material that possesses various interesting properties in the field of catalyst, electrochromism, memory devices, and sensors. Among them, tungsten trioxide ( $\text{WO}_3$ ) shows extensive application potential and has been receiving much attention due to its unique physical and chemical properties.

#### 1.1.1 Coloration

The main interest in tungsten trioxide is its coloration properties, which may be induced by a variety of methods such as electrochromism, photo-chromism, and thermo-chromism.  $\text{WO}_3$  is a kind of cathode coloration material, and the coloration process is carried out through double inserting of the electrons and cations, which can be described as:



On the one hand, it is considered that  $\text{WO}_3$  crystal changes from original semiconductor to conductor after the introduction of M atom, which can be proved by the corresponding band structures as shown in Figure 1-1. The appearance of  $\text{W}^{5+}$  cation in tungsten bronze ( $M_x\text{WO}_3$ ) is the main reason of the coloration phenomenon. On the other hand, fully oxidized  $\text{WO}_3$  crystal does not show any

coloration; however, the reduction of transparent  $\text{WO}_3$  single crystal or yellow-green  $\text{WO}_3$  powder causes blue coloration, implying that the oxygen vacancy plays a key role in this phenomenon. Therefore, the coloration of  $\text{WO}_3$  can be attributed to the electron excess localized on the  $\text{W}^{5+}$  ions. Furthermore, the oxygen vacancies have been postulated as the color center and the corresponding experimental evidence for its significance to electrochromic performance has been extensively studied. The coloration properties of tungsten trioxide are strongly dependent on the concentrations of oxygen vacancies.

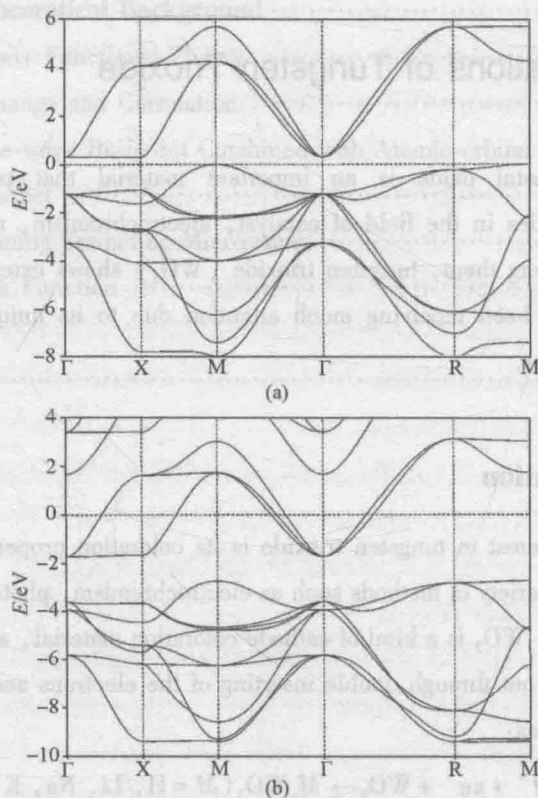


**Figure 1-1** Band structures of (a)  $\text{WO}_3$  and (b)  $\text{NaWO}_3$  along a path in typically reciprocal space for the cubic structure [All the energies are corresponding to the Fermi level.]

According to the experimental research,  $\text{WO}_{3-x}$  surfaces exhibit various chromic properties at different levels of oxygen deficiency; when  $x < 0.3$ , the

surface remains transparent and dielectric; when  $0.3 < x < 0.5$ , it exhibits blue and conductive; when  $x > 0.5$ , the surface is metallic and conductive.

### 1.1.2 Gas Sensors

Metal oxides are generally used as gas sensitive materials due to their reproducibility and typical surface properties are suitable for gas detection.  $\text{WO}_3$  is one potential candidate of gas sensors. Stoichiometric  $\text{WO}_3$  turns into non-stoichiometric  $\text{WO}_{3-x}$  under high-temperature treatment with some lattice oxygen taking off, forming a typical  $n$ -type semiconductor that the majority charge carrier is electrons. The sensor performance of  $\text{WO}_3$  material is directly related to the chemical adsorption of gas molecules on its surface. For instance, when  $\text{WO}_3$  is exposed in the air, the  $\text{O}_2$  molecules adsorb on the surface and the chemically adsorbed oxygen species  $\text{O}_2^-$ ,  $\text{O}_2^{2-}$  and  $\text{O}^{2-}$  are produced at different temperatures. The charge transfer between the adsorbed oxygen and the  $\text{WO}_3$  surface can be expected, and in the meanwhile the surface conductivity changes.

Shaver et al. first reported the gas sensing properties of  $\text{WO}_3$  to  $\text{H}_2$  and other gases including  $\text{N}_2\text{H}_4$ ,  $\text{NH}_3$ , and  $\text{H}_2\text{S}$ , etc. In addition, it has been found that  $\text{WO}_3$  material is also sensitive to other gases, especially shows excellent response to the toxic gas  $\text{NO}_x$ —typically  $\text{NO}_2$  and  $\text{NO}$ , because the W atom in  $\text{WO}_3$  surface is found to be with different oxidation states ( $\text{W}^{5+}$ ,  $\text{W}^{6+}$ ) which can improve the oxidizing ability of  $\text{NO}_x$  molecules on the  $\text{WO}_3$  surface. Tomchenko et al. prepared  $\text{WO}_3$  film sensor with different thickness that contains  $\text{Bi}_2\text{O}_3$  dopant by using traditional screen printing technology, and their tests demonstrate that  $\text{WO}_3$  exhibits good response to low-concentration of  $\text{NO}$  at the temperature of  $100 \sim 300$  °C. The prominent sensitivity of tungsten trioxide to the toxic gases ( $\text{NO}$ ,  $\text{H}_2\text{S}$  and so on) makes it possible to detect those environmentally-unfriendly gases. Thus, the tungsten trioxide has an important application in the field of trace gas treatment and environmental monitoring.

### 1.1.3 Photo-catalytic Degradation

In recent years, there has been growing interest in the heterogeneous photo-catalysis of semiconductor catalyst as a promising technology for the environmental purification and solar energy conversion. Compared with other methods, photo-catalysis has some advantages such as high efficiency, energy saving, non-toxic, no secondary pollution, etc.; as well as it exhibits wide applications in the fields of wastewater treatment and water advanced treatment.

Previous studies mainly focus on the titanium dioxide ( $\text{TiO}_2$ ) due to its high efficiency and stability; however, since it has a large band gap (about 3.2 eV), the transformation efficiency of the visible light is lower than 4%. With respect to  $\text{TiO}_2$ ,  $\text{WO}_3$  may have higher transformation efficiency due to the lower band gap (2.4 ~ 2.9 eV). Wang et al. reported the photo-catalysis properties of nanocrystal and amorphous  $\text{WO}_3$ . Their results indicate that the productivity of photo-catalytic degradation increases along with the presence of oxygen vacancy and the reduction of amorphous amount in  $\text{WO}_3$  film. Additionally,  $\text{WO}_3$  shows high efficiency and selectivity to many catalytic reactions and it has wide applications in the fields of chemical and petroleum chemical industry. For example, it can oxidize benzene and toluene into maleic anhydride and benzaldehyde, respectively. Many studies indicate that the  $\text{WO}_3$  exhibits good catalytic performances in hydrogenation, dehydrogenation, hydrocarbon isomerization, alkylation and many other reactions, etc. However, because the band gap of  $\text{WO}_3$  is not large, the redox capacity and photo-catalytic activity are not good enough. Therefore, many efforts have been paid to improve the catalytic activity of this important material.

### 1.1.4 Water-splitting Electrode

There has been considerable interest in using solar energy to produce hydrogen by photo-electrolysis of water for a long time. Especially, Fujishima and

Honda found the generation of hydrogen in the process of illuminating  $\text{TiO}_2$  to split water, which reveals the possibility of producing hydrogen by means of decomposing water. There are several factors involved in the choice of a semiconducting anode: (1) it must be chemically inert; (2) the most important factor is that the semiconductor must have an appropriate band gap which makes the best use of the solar energy (Figure 1 - 2); (3) it must match with the cathode to form a system which allows an effective conversion of solar energy to electrical or stored chemical energy. Up to date, many semiconductors have been investigated in the photo-electrolysis of water, including  $\text{TiO}_2$ ,  $\text{SrTiO}_3$ ,  $\text{SnO}_2$ , and so on. However, none of them provide a good match to the solar spectrum due to their big band gap (larger than 3.1 eV). Therefore, new classes of semiconductor materials have been taken into account in order to make better use of the visible light. Among them, tungsten trioxide ( $\text{WO}_3$ ) is a potential candidate since it can capture approximately 12% of the solar spectrum and can adsorb light in the visible spectrum up to 500 nm. Given its band gap ( $E_g = 2.6 \text{ eV}$ ),  $\text{WO}_3$  is a more suitable material for photo-electronic water splitting than  $\text{TiO}_2$  ( $E_g = 3.0 \sim 3.2 \text{ eV}$ ).  $\text{TiO}_2$  adsorbs only in the ultraviolet region of the spectrum and captures approximately 4% of solar irradiation. The theoretical maximum conversion efficiency of solar energy into  $\text{H}_2$  is only 2.2% in a photo-electro-chemical water-

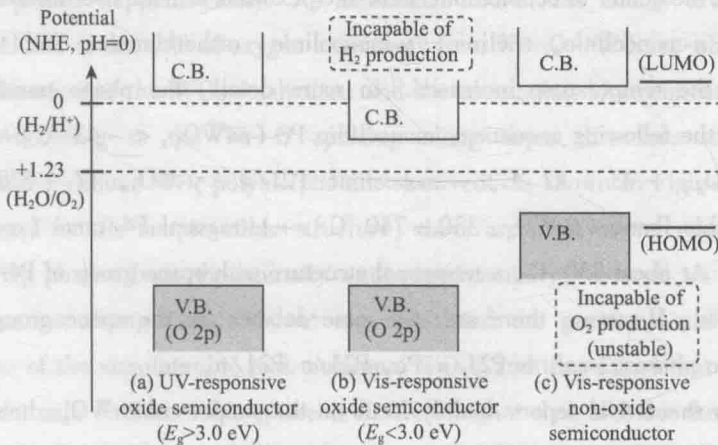


Figure 1 - 2 Energy levels of various semiconductors

splitting device using  $\text{TiO}_2$  as a photo-anode and is approximately 4.8% using  $\text{WO}_3$  as a photo-anode.  $\text{WO}_3$  exhibits high resistance against photo-corrosion and good chemical stability in acidic aqueous solutions ( $\text{pH} < 4$ ) under solar illumination. Therefore, in recent years, much effort has been focused on to improve the incident photo-to-electron conversion efficiency of  $\text{WO}_3$  photo-anode.

## 1.2 Research Progress in $\text{WO}_3$ Bulk

Similar to the structure of  $\text{ReO}_3$ , the ideal cubic  $\text{WO}_3$  crystal is originated from the cubic perovskite  $\text{ABO}_3$  structure with the missing of A atom. The basic building block of  $\text{WO}_3$  bulk is a simple cubic perovskite-type unit with W atom occupying the center of an octahedron, and the octahedron is corner-sharing with another one. All the W and O atoms are six- and two-coordinated in various  $\text{WO}_3$  crystals. Figure 1 - 3 displays the crystalline structure of  $\text{WO}_3$ . Some studies based on X-ray diffraction measurements demonstrate that  $\text{WO}_3$  prepared in experiments is usually a series of polymorphs. Like other metal oxides, the phase transitions of  $\text{WO}_3$  crystal take place during annealing and cooling. The distortion of the  $\text{WO}_6$  octahedron is observed, and as a result of the displacement of W atom away from the center of octahedron, bulk  $\text{WO}_3$  exhibits at least five different phases including  $\epsilon$ -monoclinic, triclinic,  $\gamma$ -monoclinic, orthorhombic, and tetragonal phase as the temperature increased. In more detail, the phase transformation occurs in the following sequence: monoclinic  $P_c$  ( $\epsilon$ - $\text{WO}_3$ ,  $< -43$  °C)  $\rightarrow$  triclinic  $P1$  ( $\delta$ - $\text{WO}_3$ ,  $-43 \sim 17$  °C)  $\rightarrow$  monoclinic  $P21/n$  ( $\gamma$ - $\text{WO}_3$ ,  $17 \sim 330$  °C)  $\rightarrow$  orthorhombic  $Pmnb$  ( $\beta$ - $\text{WO}_3$ ,  $330 \sim 740$  °C)  $\rightarrow$  tetragonal  $P4/nmm$  ( $\alpha$ - $\text{WO}_3$ ,  $> 740$  °C). At about 830 °C, a tetragonal structure with space group of  $P4/ncc$  may be observed. However, there are still some debates for the space groups of the monoclinic phases, such as  $P21/a$ ,  $P_c$ ,  $P21/c$ ,  $P21/n$ , etc.

Early theoretical reports mainly focus on the simple cubic  $\text{WO}_3$ ; however, in this crystalline phase, a single electron occupies in the  $e_g$  orbital, which gives rise to a second-order Jahn-Teller distortion and therefore the cubic  $\text{WO}_3$  structure is

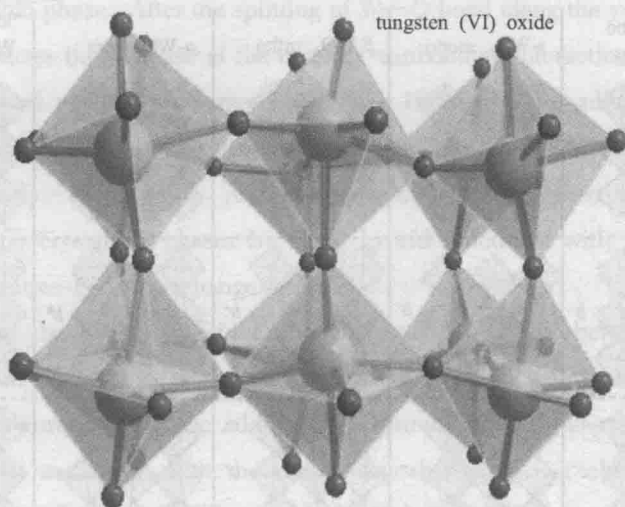


**Figure 1 – 3** Schematic structure of corner-sharing network of  $\text{WO}_6$  octahedron in  $\text{WO}_3$  crystal [ The big spheres stand for the W atoms, while the small spheres denote the O atoms. ]

unstable. Actually, this simple cubic  $\text{WO}_3$  crystalline phase is difficult to be observed in the experiment, except in the  $\text{WO}_3$  film. Theoretically, we will see that the energy differences between the simple cubic  $\text{WO}_3$  and other distorted phases are very small, indicating that the structural transformation between different phases happens easily. As mentioned above, the energy divergence is mostly related to the shift of oxygen atom away from W—O—W line, which results in the distortion of the  $\text{WO}_6$  octahedron and the alternating arrangement of W—O bond. According to the W—O splitting along three directions at different temperature, various  $\text{WO}_3$  polymorphs are observed, as shown in Figure 1-4.

Except for the simple cubic structure, there are also several reports on the other  $\text{WO}_3$  phases both theoretically and experimentally, as well as the phase transformation among them. Corûet al. calculated the geometry and electronic structures of the simple cubic and tetragonal  $\text{WO}_3$ , and they found that the energy of  $\text{WO}_3$  formula unit for cubic phase is 0.8 eV higher than that for the tetragonal one, owing to the elongating of W—O covalent bond. Experimentally, Vogt et al. investigated the high-temperature phases ( orthorhombic  $\beta\text{-WO}_3$  and tetragonal

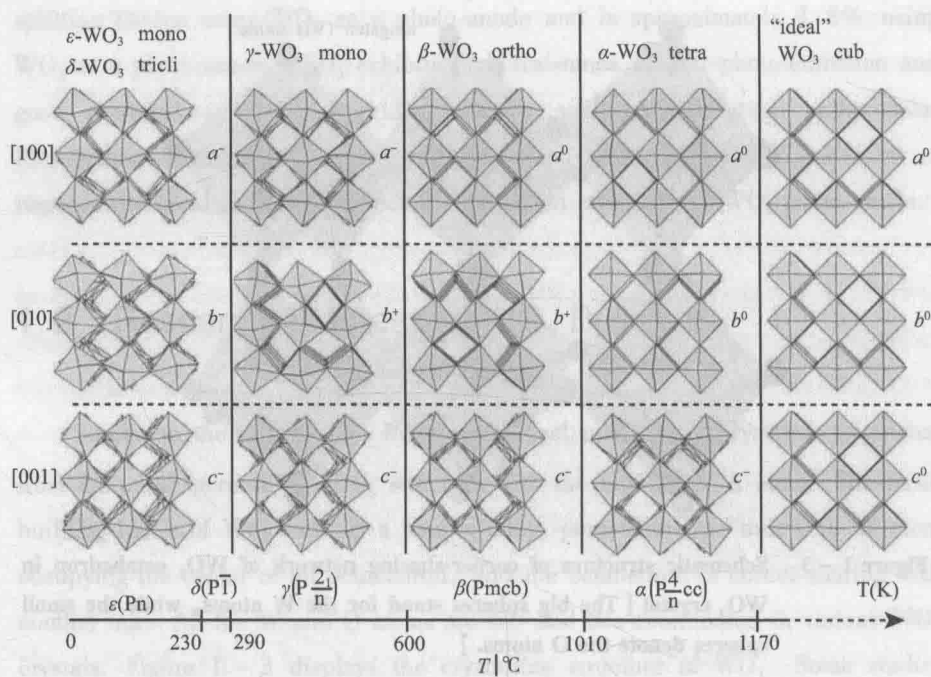


**Figure 1-4** Tilt patterns and stability temperature domains of the different polymorphs of  $\text{WO}_3$

$\alpha\text{-WO}_3$ ) of  $\text{WO}_3$  with the help of high-resolution neutron powder diffraction. Their results further confirmed that the temperature induced phase transitions in  $\text{WO}_3$  can be rationalized in terms of the changes in the tilt direction of  $\text{WO}_6$  octahedron and/or off-center displacements of the tungsten cations.

Besides, the structural distortion has a major impact on the electronic properties, such as the band gap of  $\text{WO}_3$  bulk. First-principles studies of Chatten et al. illustrated that the electronic structure of  $\text{WO}_3$  bulk is critically dependent on the splitting of W—O bond along each direction. The cubic  $\text{WO}_3$  has a small band gap of 0.69 eV; while the W—O bond only splits along  $z$  axis, i. e. in the tetragonal phase, the band gap enlarges slightly (0.71 eV); as for the orthorhombic one, the W—O bond further splitting along the  $y$  direction, making its band gap increase to 1.50 eV. Therefore, the obvious splitting of W—O bond along the  $y$  direction is the dominant factor in determining the band gap of  $\text{WO}_3$ .